

# Estimation of Soiling Losses in Unlabeled PV Data

Bennet Meyers<sup>1,2</sup>

<sup>1</sup> SLAC National Accelerator Laboratory, Menlo Park, CA, 94025, USA

<sup>2</sup> Stanford University, Stanford, CA, 94305, USA

**Abstract**—We provide a methodology for estimating the losses due to soiling for photovoltaic (PV) systems. We focus this work on estimating the losses from historical power production data that are unlabeled, *i.e.* power measurements with time stamps, but no other information such as site configuration or meteorological data. We present a validation of this approach on a small fleet of typical rooftop PV systems. The proposed method differs from prior work in that the construction of a performance index is not required to analyze soiling loss. This approach is appropriate for analyzing the soiling losses in field production data from fleets of distributed rooftop systems and is highly automatic, allowing for scaling to large fleets of heterogeneous PV systems.

**Index Terms**—photovoltaic systems, solar energy, distributed power generation, energy informatics, machine learning, statistical learning, unsupervised learning, soiling, unlabeled data

## I. INTRODUCTION

Soiling can cause significant energy yield reduction in photovoltaic (PV) systems, as high as  $-1\%/day$ , but the effects are quite variable and impacted by many factors from system geometry to local climate conditions to nearby industry and agriculture [1]. Quantifying the losses due to soiling is important for understanding and mitigating this effect, which in turn improves the overall reliability and dependability of PV as an energy generation source. This importance is seen in the dedicated subarea for soiling at this conference, as well as the strong emphasis on soiling at other events such as the yearly PV Reliability Workshop hosted by NREL. Largely absent from this conversation, however, is quantification of the impacts of soiling in large fleets of heterogeneous, distributed PV systems, which comprised over 40% of the installed capacity in 2020 [2]. The reason for this is a technical one: it is very difficult to analyze soiling trends without a reliable reference, and the unlabeled nature of distributed PV data make generating this reference difficult or impossible.

In this work, we present a methodology, based on recent research on machine learning for signal processing, that extracts estimates of system soiling losses from *unlabeled* production data. This work eliminates the requirement of constructing a performance index to analyze soiling loss and is highly automated, thus enabling the large-scale analysis of fleets of thousands of heterogeneous systems. The proposed approach is based on an implementation of the *signal decomposition* (SD) framework [3].

This material is based on work supported by the U.S. Department of Energy’s Office of Energy Efficiency and Renewable Energy (EERE) under the Solar Energy Technologies Award Number 38529.

Our approach takes unlabeled PV power generation measurements as an input and returns an estimate of the soiling loss over time, given as a percent loss relative to the unsoiled performance. This trend may be used to calculate secondary statistics such as the total energy loss or seasonal loss patterns. We validate this method on synthetic data, labeled data from a soiling test site, and on representative unlabeled data. The algorithm is available as a module in the Solar Data Tools package [4], [5]. This approach is uniquely suited to the analysis of fleet-scale PV systems, where it can be difficult or impossible to get suitable reference data for normalization.

## II. RELATED WORK AND CONTRIBUTIONS

We are not the first to propose a method for estimating soiling losses from PV production data [6]–[9]. As described in [8], it has been determined that a combined model of degradation, soiling, and seasonal bias outperforms estimates of each loss term separately.

In this paper, we build upon previous work in a few ways. First, we propose a clear unified signal model (implemented as an SD problem) to describe the underlying components, rather than invoking iterative heuristics. Second, the use of the extensible SD framework allows for the expression of component classes that are designed specifically for this application. Third, our approach estimates soiling losses from unlabeled system power generation time series data, without the need to construct a performance index (PI). As discussed in the introduction, this unlocks the analysis of around 40% of the installed PV capacity in the United States. An example of a PI constructed from data labels and an unlabeled daily energy signal are shown in figure 1. The proposed method allows for the analysis of *both* unlabeled and labeled data. Labeled data will provide more accurate results, when available, but reasonable estimates may be obtained when such labels are unavailable.

## III. METHODS

We construct an SD problem [3] that models the decomposition of measured daily PV system energy or normalized energy (*i.e.*, a performance index, “PI”) into a number of components, one of which represents the soiling loss in the system. This approach can be thought of as an *unsupervised* machine learning (ML) method for finding structure in time series data, similar to model-based clustering methods like Gaussian mixture models [10, §14.3.7]. Unlike supervised ML, there is no “training” of the method; we simply design the mathematical optimization problem, input the data for



Fig. 1. A comparison of labeled data (top) and unlabeled data (bottom) from a single PV system in a desert environment.

analysis, and receive the soiling estimate. In this section, we describe the data preparation, SD formulation, and validation procedure. Finally, we briefly describe a procedure for utilizing the estimate of system soiling to “correct” the measured power data.

#### A. Data preparation

The proposed method of signal decomposition operates on a discrete daily time series representing raw or normalized daily system energy production, which we refer to as “unlabeled” and “labeled” data respectively. The purpose of generating a performance index is to remove known sources or variation in data, particularly due to available irradiance and operating temperature, and is a typical analytical approach for PV performance analysis, but requires additional knowledge about the system and its operating environment beyond real power production.

The raw data may be any measurements of PV system power or energy production indexed in time. This may be 1-minute measurements of instantaneous power, 15-minute interval averaged power, or daily energy production. If starting from high-frequency power measurements, one simply integrates to get the daily energy production. If one wishes to construct a PI, you then normalize by expected daily energy at this time.

When starting from sub-daily measurements, any prefiltering step may be applied, and rejected days can have their values replaced with NaN values (which we represent as ? in our notation). The SD framework optimally handles missing data points, so there is no need to use corrupted or untrustworthy data nor replace such data with interpolated values.

In this paper, we validate on both synthetic and real data. As described in §III-C0a, the synthetic data is already a daily time-series (a normalized PI), so no preprocessing is required. For the real data, which has a 5-minute measurement interval,

we use the data cleaning and filtering tools provided in Solar Data Tools [4], [5], and replace days that do not pass the quality check with ? values. After obtaining a representation of daily energy production (possibly with missing values), the signal is scaled so the 95<sup>th</sup> percentile is equal to 1. This is our input to the *signal decomposition problem* (SD problem). We do not construct a performance index on the real data and instead analyze the raw energy signal.

#### B. SD problem formulation

Utilizing the notation of signal decomposition defined in [3], we say that our data for the SD problem is a signal  $y \in (\mathbf{R} \cup \{?\})^{T \times p}$  with length  $T$  equal to the number of days in the data set and measurement dimension  $p = 1$ . In this case, because the measurement dimension is equal to 1,  $y$  may also be thought of as a column vector of length  $T$ . We model the signal  $y$  as the composition of  $K = 4$  components,  $x^1$  to  $x^4$ , the sum of which must be equal to the signal  $y$  at the entries that do not contain missing values, or in other words,

$$y_t = x_t^1 + x_t^2 + x_t^3 + x_t^4, \text{ for } t \in \mathcal{K},$$

where  $\mathcal{K}$  is the set of time indices that do not contain missing values (the “known” set). The four components are defined in the SD model by their cost functions  $\phi_k(x^k)$  for  $k = 1, \dots, 4$ . (We drop the superscript  $k$  on  $x$  to keep the notation lighter when not distinguishing between particular components.) As we will see, the last component,  $x^4$ , will represent the soiling signal which we wish to estimate from the data. The other three components represent other processes which impact the energy production of the system.

a) *Component definitions:* The first component represents the residual of the model, and it is taken to be the quantile cost function [11], [12],

$$\phi_1(x) = \mathbf{quant}_\tau(x) = \sum_{t=1}^T (1/2) |x_t| + (\tau - 1/2)x_t,$$

where  $\tau \in (0, 1)$  is a parameter. When  $\tau < 0.5$ , positive residuals are preferred to negative residuals, and vice versa when  $\tau > 0.5$ . When working with raw energy data, we set  $\tau = 0.85$ , which strongly prefers negative residuals, accounting for the fact that we have not normalized for weather effects, and clouds tend to reduce rather than increase the system energy product. When operating on normalized, PI data (such as the synthetic data set in this paper), we set  $\tau = 0.5$  since we expect the deviations from the expected output to be symmetric, or at the very least more symmetric than when no normalization is performed.

The second component is a seasonal term, which is smooth and periodic each year,

$$\phi_2(x) = \begin{cases} \lambda_2 \|D_2 x\|_2^2 & x_t = x_{t+Y}, \text{ for } t = 1, \dots, T - Y \\ \infty & \text{otherwise,} \end{cases}$$

where  $D_2 \in \mathbf{R}^{(T-2) \times T}$  is the second-order discrete difference operator. (See, for example, [13, §6.4] for information on difference matrices.)  $\lambda_2$  is a weighting parameter, and  $Y = 365$  is

the period of the component. The normalization of the energy signal affects the expected amplitude of this component. That is, we would expect raw energy data to have a larger seasonal component than normalized data. The component definition presented here covers both cases well and is not sensitive to the amplitude of the component.

The third component represents the bulk, long-term degradation rate, and is given by

$$\phi_3(x) = \begin{cases} 0 & x_0 = 0 \text{ and } x_t = mt + b \text{ for } t = 1, \dots, T \\ \infty & \text{otherwise,} \end{cases}$$

for some values of  $m$  and  $b$ . This just constraints the component to be linear with respect to time with an initial value equal to zero. We have chosen a linear degradation model due to its popularity in the literature, but we note that other trend models could be employed within the SD framework, *e.g.*, a smooth, monotonically decreasing signal. Note that the third component does not include a weight parameter, as the penalty function only takes on values of zero or infinity.

The fourth and final component represents what we are interested in measuring, the soiling losses in the system. This cost is defined as,

$$\phi_4(x) = \begin{cases} \ell_{4a}(x) + \ell_{4b}(x) + \ell_{4c}(x) & x \leq 0 \\ \infty & \text{otherwise,} \end{cases}$$

where the summed functions are

$$\begin{aligned} \ell_{4a} &= \lambda_{4a} \|D_2 x\|_1 \\ \ell_{4b} &= \lambda_{4b} \sum_{t=0}^T (-x_t) \\ \ell_{4c} &= \lambda_{4c} \mathbf{quant}_\tau(D_1 x) \end{aligned}$$

with parameters  $\lambda_{4a}$ ,  $\lambda_{4b}$ , and  $\lambda_{4c}$ .  $D_2$  is again the second-order discrete difference operator, and  $D_1$ , similarly, is the first-order difference. The quantile cost parameter  $\tau$  is taken to be 0.9 here. This cost is a composite of simpler functions, which combine to select for signals with the following characteristics:

- non-positive (soiling can only reduce the system power)
- sparse in second-differences (*i.e.*, piecewise linear)
- with values “close” to zero (in sum-absolute sense)
- a preference for more values with a negative slope than a positive one (*i.e.*, a tendency towards slow degradation and quick recovery).

Component cost  $\phi_4$  demonstrates the *extensibility* of the SD framework. We are able to build up a complex cost function from smaller units and design it in a way to capture domain knowledge about the component.

*b) SD parameters:* The SD problem formulating includes four parameters,  $\lambda_2$ ,  $\lambda_{4a}$ ,  $\lambda_{4b}$ , and  $\lambda_{4c}$ . These parameters are tunable, and different values can greatly effect the characteristics and quality of the resulting decomposition. A deep discussion on the role of parameters in SD problems can be found in [3, §2.6]. While a method is provided in [3, §2.7] for selecting optimal parameter values, we find that in this context it makes more sense to rely on the practical experience of the

TABLE I  
SD PROBLEM PARAMETERS

param.	value	description
$\lambda_2$	$5 \times 10^2$	stiffness of seasonal baseline
$\lambda_{4a}$	2	effects number of soiling component breakpoints
$\lambda_{4b}$	$3 \times 10^{-2}$	penalizes large values of soiling component
$\lambda_{4c}$	$2 \times 10^{-1}$	encourages asymmetric rates in soiling component

analyst. In other words, we have found values that work well in many cases, and a small amount of hand-tuning is accepted in other cases. A description of these parameters and their default values are given in table I.

*c) Solution method:* The SD problem is convex (inequality-constrained quadratic program [14, §4.4]) and of modest size (around 2.1k variables for 3-year data set to around 15k variables for a 10-year data set), so we simply use CVXPY [15], [16] and the commercial Mosek solver [17], which is sufficient for research purposes. An implementation of the algorithm described in [3] would allow for the removal of the dependence on Mosek and is an area for future work.

### C. Validation

The most desirable method of validation for an unsupervised machine learning algorithm such as the methods described in this paper would be access to real PV system production data that has been hand-labeled with soiling trends. Because this is difficult to obtain or generate, we take a multi-modal approach to validation in this paper, with three different approaches to validation, described below, ordered by how well labeled the data source is.

*a) Synthetic data:* We follow the methods published in [8] to evaluate the performance of the algorithm on synthetic data that represents normalized energy productions. This approach generates random realizations of PI signals, with components drawn from pre-defined statistical models. The synthetic data model includes a ‘seasonal’ term which represents the seasonal variation in performance. Normalization with a performance index is typically expected to lower this seasonal variation, but it does not fully remove it. The noise term in the model is Gaussian white noise, representing the assumption that a PI signal normalized for weather phenomenon. We therefore set  $\tau = 0.5$  in  $\phi_1$  of the SD formulation to reflect the expectation of symmetric residuals.

Because the synthetic model explicitly models the system soiling losses, we are able to directly assess the ability of the SD soiling algorithm to estimate the hidden soiling signal. We select *mean-absolute error* (MAE) as a summary error metric for comparing the known synthetic soiling loss to the SD estimate, which is preferred over *root-mean-square error* when the errors are not expected to be normally distributed [18, §6.1.2]. Because analysts often want to be able to estimate soiling *rates* on a PV system, in addition to understanding the total energy loss, we calculate the MAE on both the soiling loss component and the first-order difference [19] of the loss,

which we call the soiling rate. Finally, we note a small error in estimate of a cleaning event (*i.e.*, one day before or after the true event) is of small consequence to the analyst but will result in very large error values, especially for the analysis of soiling rates. Therefore, we introduce a third summary statistic which is the MAE of *filtered* soiling rate, which simply selects for time periods when both the synthetic soiling component and the SD estimate agree that the instantaneous soiling rate is negative, *i.e.*, neither component is currently in a cleaning event. This final metric provides useful insight into the ability of the algorithm to accurately estimate the rate of soiling loss between cleaning events.

b) *Labeled production data*: Labeled soiling data was presented in [20] and analyzed for soiling trends. We leverage these published results to validate the SD soiling algorithm on the *unlabeled* power production data. For this power, we ignore the reference system, treating the test system as an unlabeled data source, and estimate the soiling losses of the test system using the SD formulation. Then we compare results of the proposed method to the results from [20]. We calculate the same three error metrics for this data set, as described previously for the synthetic data.

c) *Unlabeled production data*: We demonstrate the application of the SD soiling method on a selection of 50 PV systems, with only access to measured real power. There is no known soiling trend to compare to in this case. Instead, this represents what we see as a typical use case, and we show how outlier sites may be identified.

#### D. Soiling correction for downstream analysis

We briefly note that the estimate of soiling loss may be used to “correct” for soiling for other analysis. For example, we note in two other papers submitted to this conference [21], [22], that it is beneficial to account for soiling in production PV data prior to analyzing shade losses. We provide a simple procedure for doing this correction here.

The soiling loss component is a daily signal representing the fractional loss in daily energy from soiling, typically between 0 and 1. Therefore, the expected power output of the system in the absence of soiling would be the measured power divided by the instantaneous soiling loss. The Solar Data Tools implementation of the methods described in this paper includes a feature for automatically performing this correction.

## IV. RESULTS

### A. Synthetic data

Following the scenario generation procedure defined in [8, §II-D], we define six generative model configurations, with different levels of soiling, seasonality, and noise. These scenarios are briefly described in II. Two characteristic examples of the synthetic PI signals are shown in figure 2, and the SD estimates of the soiling trends are compared to the true values in figure 3. The error metric for these two examples is given in table III. The soiling rate were on average around -0.001 for the first example and -0.0005 for the second example.

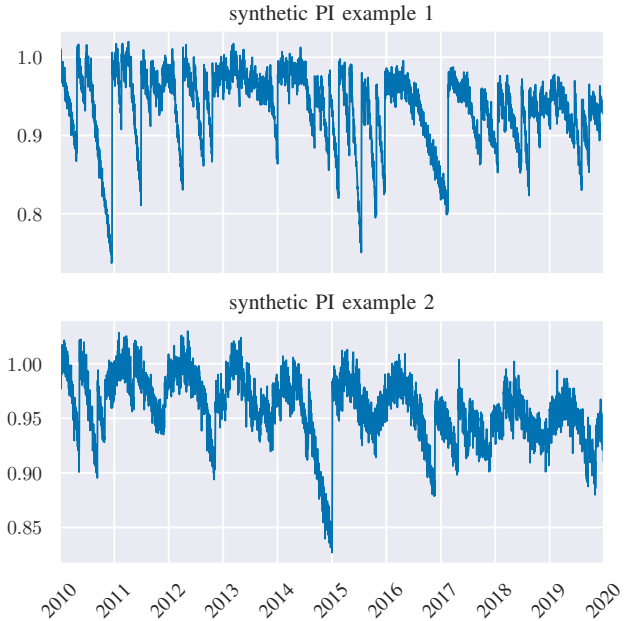


Fig. 2. Two typical synthetic soiling signals generated by NREL software. The top signal is drawn from scenario 1 and the bottom from scenario 2.



Fig. 3. Comparison of the actual and estimated soiling components in the two synthetic examples shown in figure 2.

TABLE II  
SYNTHETIC DATA SCENARIOS

number	name	description
1	normal	soiling rates ( $sr$ ) uniform in $[0, 0.003]$
2	M soil, H season	$sr \in [0, 0.001]$ , double seasonal amplitude
3	M Soil, H noise	$sr \in [0, 0.001]$ , double noise amplitude
4	seasonal cleaning	$sr \in [0, 0.005]$ , cleaned seasonally
5	M soil	$sr \in [0, 0.005]$
6	L soil	$sr \in [0, 0.001]$

TABLE III  
ERROR METRICS FOR TWO SYNTHETIC SOILING EXAMPLES

	loss MAE	rate MAE	filtered rate MAE
Ex. 1	0.008698	0.002257	0.000379
Ex. 2	0.005366	0.000919	0.000202

We sample the 6 scenarios 10 times each, and we solve the associated SD problem for each of the 60 realizations. Finally, we calculate the three error metrics for each realization. The distribution of loss MAE is given in figure 4; the distribution of rate MAE is given in figure 5, and the distribution of the filtered rate MAE is given in figure 6.

### B. Labeled data

The labeled performance index and corresponding unlabeled energy signal was previously shown in figure 1. In figure 7, these signals are overlaid with the “denoised” SD signal estimate, *i.e.*, the sum of the estimated components excluding the first residual term. Note how the SD model for the PI assumes symmetric residuals ( $\tau = 0.5$ ) while the model for the energy signal assumes highly asymmetric residuals ( $\tau = 0.85$ ). Figure 8 shows the comparison between the soiling loss components estimated from the PI and from the unlabeled energy signal. Taking the loss component derived from the PI signal as groundtruth, we then calculate the three error metrics for the energy-derived soiling estimate. The loss MAE

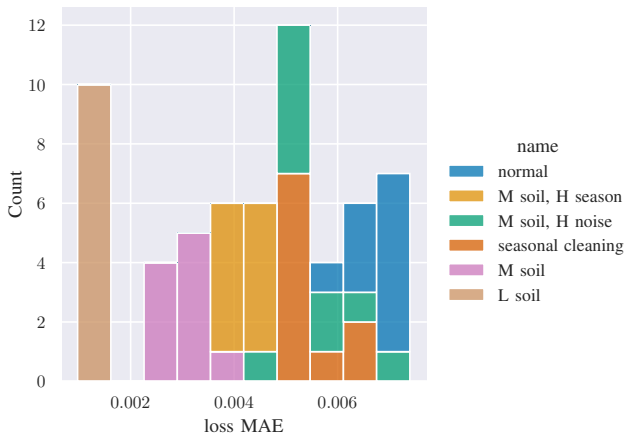


Fig. 4. Distribution of loss MAE for the 60 realizations, labeled by scenario.

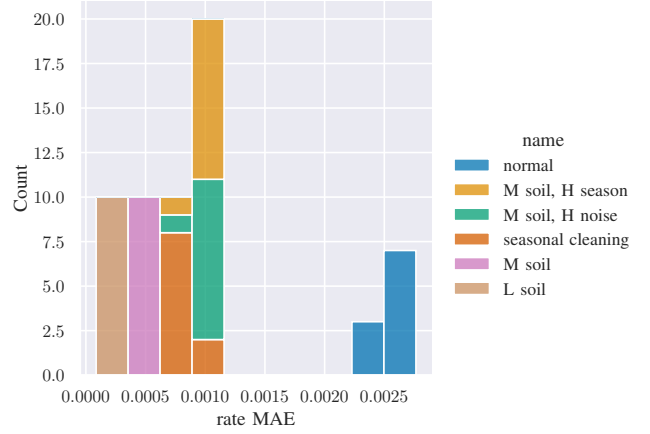


Fig. 5. Distribution of rate MAE for the 60 realizations, labeled by scenario.

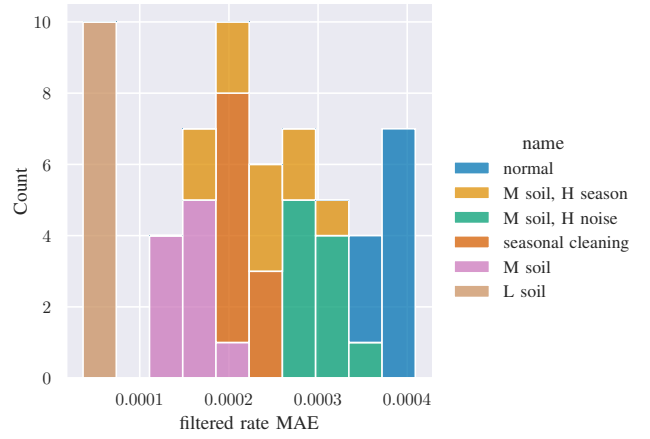


Fig. 6. Distribution of the filtered rate MAE for the 60 realizations, labeled by scenario. This metric accurately captures how closely the SD method estimated the loss rates during soiling periods.

is 0.042558; the rate MAE is 0.004734, and the filtered rate MAE is 0.001756.

We find that the analysis of the unlabeled energy produces an estimate of soiling losses that agrees well with the PI-derived estimate. We observe that the unlabeled analysis does worst around days 125–200, which was particularly rainy and cloudy. This lack of clear sky baseline during this period is seen to negatively impact the soiling estimate. However, with additional years of data, this may be improved due to the seasonal structure in the second component.

### C. Unlabeled data

In [21], we present a preliminary shade loss analysis of an unlabeled rooftop PV data set. As described in that manuscript, the shade analysis depends on first estimating and correcting the soiling losses in the signal. A view of the soiling signal decomposition for one system in this data set is shown in figure 9, and the soiling component in isolation is shown in figure 10.

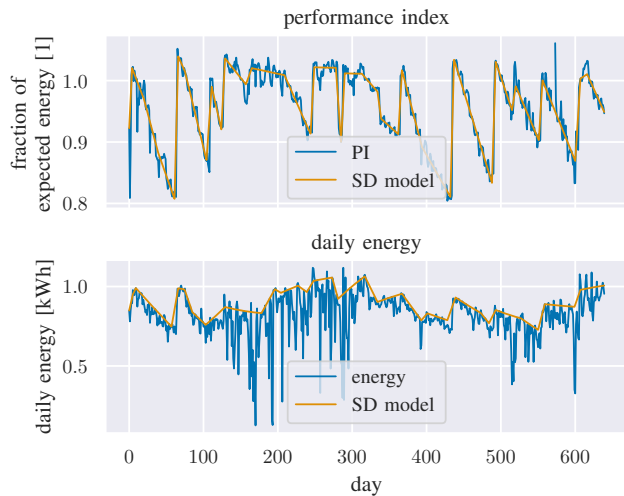


Fig. 7. PI and energy signals for the labeled soiling test system, with the denoised SD estimates overlaid in orange.

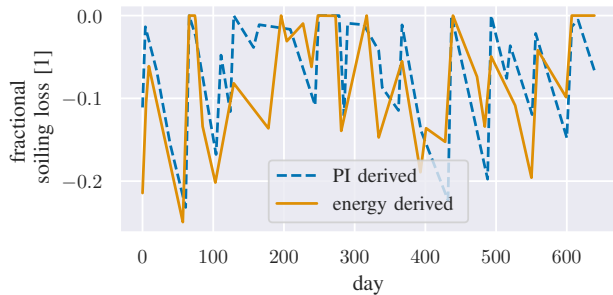


Fig. 8. Comparison of the estimated soiling loss component from the PI signal and the unlabeled energy signal.

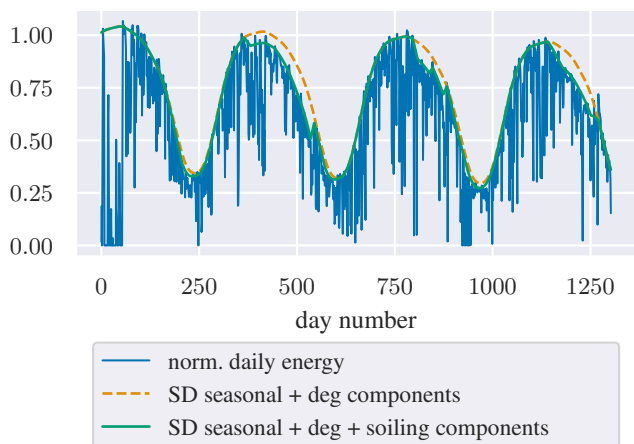


Fig. 9. An illustration of the soiling decomposition results for the unlabeled rooftop PV data discussed in [21]. The soiling trend is estimated to be the difference between the orange and green trends.

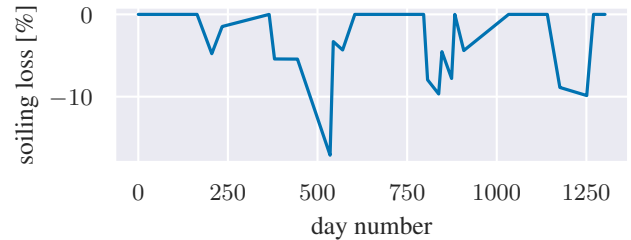


Fig. 10. The isolated soiling trend for the unlabeled data analysis.

## V. CONCLUSIONS

We present a methodology, based on the signal decomposition (SD) framework, for estimating soiling losses PV system production data, *i.e.*, time series measurements of generated real power or energy, typically over multiple years. Unique to this work is the capability to estimate soiling losses in raw, unlabeled power/energy data, rather than requiring a performance index. By utilizing the extensibility of the SD, we are able to design a signal decomposition model that is bespoke to the problem of estimating soiling losses. This results in a robust model for the soiling loss component,  $x^4$ , as well as adjustable residual component,  $x^1$ , that is able to model both unlabeled ( $\tau = 0.85$ ) and labeled ( $\tau = 0.5$ ) data. The ability to analyze unlabeled PV data potentially unlocks huge potential in the form of fleet-scale datasets of heterogeneous, distributed PV systems, which typically have internet-connected power electronics which generate time series of real power, but lack correlated meteorological measurements and possibly accurate system models. A software implementation is available in the Solar Data Tools package [4], [5] and a demonstration notebook of the code usage is available online [23].

## ACKNOWLEDGMENTS

The author would like to thank Stephen Boyd, Justin Luke, Elsa Kam-Lum, Mayank Malik, and the entire GISMo Team at SLAC National Accelerator Laboratory for their input and feedback on this work. I also recognize the Seaborn plotting package for Python, which made the figures possible [24].

## REFERENCES

- [1] K. Ilse, L. Micheli, B. W. Figgis, K. Lange, D. Daßler, H. Hanifi, F. Wolfertstetter, V. Naumann, C. Hagendorf, R. Gottschalg, and J. Bagdahn, "Techno-economic assessment of soiling losses and mitigation strategies for solar power generation," *Joule*, vol. 3, no. 10, pp. 2303–2321, 2019. [Online]. Available: <https://www.sciencedirect.com/science/article/pii/S2542435119304222>
- [2] M. Davis, C. Smith, B. White, R. Goldstein, X. Sun, M. Cox, G. Curtin, R. Manghani, S. Rumery, C. Silver, and J. Baca, *U.S. Solar market insight executive summary, 2020 year in review*. Wood Mackenzie and SEIA, 2021.
- [3] B. Meyers and S. Boyd, "Signal decomposition using masked proximal operators," pp. 1–60, feb 2022. [Online]. Available: <http://arxiv.org/abs/2202.09338>
- [4] B. Meyers, E. Apostolaki-Iosifidou, and L. Schelhas, "Solar data tools: Automatic solar data processing pipeline," in *2020 47th IEEE Photovoltaic Specialists Conference (PVSC)*, 2020, pp. 0655–0656.
- [5] B. Meyers, "solar-data-tools," may 2022. [Online]. Available: <http://dx.doi.org/10.5281/zenodo.6450368>

- [6] M. Deceglie, L. Micheli, and M. Muller, "Quantifying soiling loss directly from pv yield," *IEEE Journal of Photovoltaics*, vol. 8, no. 2, pp. 547–551, 2018.
- [7] Å. Skomedal, H. Haug, and E. S. Marstein, "Endogenous soiling rate determination and detection of cleaning events in utility-scale pv plants," *IEEE Journal of Photovoltaics*, vol. 9, no. 3, pp. 858–863, 2019.
- [8] A. Skomedal and M. Deceglie, "Combined Estimation of Degradation and Soiling Losses in Photovoltaic Systems," *IEEE Journal of Photovoltaics*, vol. 10, no. 6, pp. 1788–1796, nov 2020. [Online]. Available: <https://ieeexplore.ieee.org/document/9186286/>
- [9] L. Micheli, M. Theristis, A. Livera, J. Stein, G. Georghiou, M. Muller, F. Almonacid, and E. Fernandez, "Improved PV soiling extraction through the detection of cleanings and change points," *IEEE Journal of Photovoltaics*, vol. 11, no. 2, pp. 519–526, 2021.
- [10] T. Hastie, R. Tibshirani, and J. Friedman, *The Elements of Statistical Learning*, ser. Springer Series in Statistics. New York, NY: Springer New York, dec 2009. [Online]. Available: <http://ieeexplore.ieee.org/document/6727256/http://link.springer.com/10.1007/978-0-387-84858-7>
- [11] R. Koenker and G. Bassett, "Regression quantiles," *Econometrica*, vol. 46, no. 1, p. 33, jan 1978. [Online]. Available: <https://www.jstor.org/stable/1913643https://www.jstor.org/stable/1913643?origin=crossref>
- [12] R. Koenker and K. F. Hallock, "Quantile regression," *Journal of Economic Perspectives*, vol. 15, no. 4, pp. 143–156, nov 2001. [Online]. Available: <https://pubs.aeaweb.org/doi/10.1257/jep.15.4.143>
- [13] S. Boyd and L. Vandenberghe, *Introduction to Applied Linear Algebra*, 2018.
- [14] —, *Convex optimization*. Cambridge University Press, 2009.
- [15] S. Diamond and S. Boyd, "CVXPY: A Python-embedded modeling language for convex optimization," *Journal of Machine Learning Research*, vol. 17, no. 83, pp. 1–5, 2016.
- [16] A. Agrawal, R. Verschuere, S. Diamond, and S. Boyd, "A rewriting system for convex optimization problems," *Journal of Control and Decision*, vol. 5, no. 1, pp. 42–60, 2018.
- [17] E. D. Andersen and K. D. Andersen, "The Mosek Interior Point Optimizer for Linear Programming: An Implementation of the Homogeneous Algorithm," in *High performance optimization*, 2000, pp. 197–232. [Online]. Available: [http://link.springer.com/10.1007/978-1-4757-3216-0\\_{\\_}8](http://link.springer.com/10.1007/978-1-4757-3216-0_{_}8)
- [18] S. Boyd and L. Vandenberghe, "Convex Optimization," in *Cambridge University Press*, 2004.
- [19] "Numpy.diff," *NumPy v1.22 Manual*. [Online]. Available: <https://numpy.org/doc/stable/reference/generated/numpy.diff.html>
- [20] E. Kam-Lum, B. E. Meyers, D. Cosme, B. Aissa, and G. Scabbia, "Soiling Rate Determination from Referenced Systems in Desert Climate using PVInsight Soiling Algorithm," in *2021 IEEE 48th Photovoltaic Specialists Conference (PVSC)*, no. July 2019. IEEE, jun 2021, pp. 2552–2554. [Online]. Available: <https://ieeexplore.ieee.org/document/9518459/>
- [21] B. Meyers and D. F. Florez Rodriguez, "Estimation of shade losses in unlabeled PV data," *Submitted to PVSC49*, June 2022.
- [22] D. F. Florez Rodriguez and B. Meyers, "Solar panel power simulation for shade detection," *Submitted to PVSC49*, June 2022.
- [23] B. Meyers, "Soiling analysis demonstration," *solar-data-tool GitHub repository*, May 2022. [Online]. Available: [https://github.com/slaggismo/solar-data-tools/blob/shade-dev/notebooks/Soiling\\_analysis\\_demonstration.ipynb](https://github.com/slaggismo/solar-data-tools/blob/shade-dev/notebooks/Soiling_analysis_demonstration.ipynb)
- [24] M. L. Waskom, "seaborn: statistical data visualization," *Journal of Open Source Software*, vol. 6, no. 60, p. 3021, 2021. [Online]. Available: <https://doi.org/10.21105/joss.03021>